

Density of states and thermodynamic properties of a two-dimensional electron gas in a strong external magnetic field

X. C. Xie, Q. P. Li, and S. Das Sarma

*Center for Theoretical Physics and Center for Superconductivity Research, Department of Physics,
University of Maryland, College Park, Maryland, 20742-4111*

(Received 21 May 1990)

We develop a theory for the electronic density of states of a weakly disordered two-dimensional electron gas in the presence of a strong external magnetic field oriented normal to the electron layer. The disorder arises from randomly distributed charged impurity centers that interact with the electrons, in the absence of any screening, via the long-range Coulomb interaction. To mimic modulation doping in high-mobility heterostructures, the electron plane is assumed to be separated by a spacer layer from the impurity plane. The density of states is calculated using the self-consistent Born approximation for the electron-impurity scattering, retaining Landau-level coupling in the theory. The electron-impurity scattering potential is calculated in a nonlinear screening approximation where scattering and screening self-consistently determine each other. Thus, the level broadening determining the electron propagator in each Landau level is calculated by using the screened impurity potential in the self-consistent Born approximation, whereas the screened potential itself is calculated self-consistently by calculating the electron polarizability with use of the renormalized electron propagator. Screening is treated in the random-phase approximation by retaining the bubble diagrams, and the polarizability is obtained by solving the vertex function within the ladder approximation (which is consistent with the self-energy being treated in the single-site approximation). The resultant level broadening and the electronic density of states cannot easily be characterized by a single parameter, such as the zero-field mobility, which uniquely characterizes the usual short-range approximation extensively used in the literature. We find that the density of states calculated from this nonlinear, self-consistent screening theory is, in general, much smoother and flatter and the Landau-level broadening much larger than that implied in the short-range approximation. The density of states depends on the actual impurity distribution (and, *not* just on the mobility) in the system and the level broadening and screening are the oscillatory function of the chemical potential. We conclude that in many experimental situations the short-range approximation is even qualitatively wrong. We give detailed numerical results for the density of states and level broadening, and apply the theory to the calculation of thermodynamic quantities, such as electronic specific heat and magnetic susceptibility. Excellent qualitative and semiquantitative agreement with available experimental results is found.

I. INTRODUCTION

When a strong external magnetic field B is applied normal to a two-dimensional electron gas (2DEG), the system becomes quantized into a series of Landau levels (denoted by the index $N=0,1,2,\dots$, throughout this paper) whose energy E_N , in the noninteracting situation, is given by ($\hbar=1$ throughout)

$$E_N = (N + \frac{1}{2})\omega_c, \quad (1.1)$$

where,

$$\omega_c = eB/mc \quad (1.2)$$

is the cyclotron frequency and m the electron (band) effective mass. Each Landau level, denoted by the discrete index N , is highly degenerate with a macroscopic degeneracy given by $(2\pi l^2)^{-1}$ per spin unit area where $l = (c/eB)^{1/2}$ is the Landau radius or the magnetic length. Thus, for a given two-dimensional electron density N_s at $T=0$, a certain number n of Landau levels will

be occupied by electrons where n is the largest integer satisfying the inequality condition

$$N_s \leq (n/2\pi l^2), \quad (1.3)$$

with the equality being valid when n levels are exactly filled and the $(n+1)$ th level is completely empty. In general, at $T=0$ the chemical potential or the Fermi energy (E_F) will be in the $(n-1)$ th Landau level ($n=1,2,3,\dots$)

$$E_F = (n - \frac{1}{2})\omega_c, \quad (1.4)$$

except in the situations (of measure zero) when n Landau levels are *exactly* full and $E_F = n\omega_c$. Thus, in a constant magnetic field, the Fermi energy remains locked in individual Landau levels as N_s increases (decreases) and then jumps to the next higher (lower) Landau level as the next integer satisfies the inequality (1.3). The situation is similar when B is changed at a constant N_s — E_F remains locked in an individual level and then jumps to the next lower (higher) Landau level as B is increased (decreased)

beyond the next critical value determined by (1.3).

The density of states (DOS) of the noninteracting 2DEG in the presence of an external normal magnetic field is easily seen¹ to be a series of δ functions at the quantized Landau energies

$$D(E) = (2\pi l^2)^{-1} \sum_{N=0} \delta(E - E_N), \quad (1.5)$$

where the δ function sharpness reflects the complete quantization of the system as indicated by Eq. (1.1). Throughout this work we assume the electrons to be spinless fermions, neglecting the electron spin degeneracy completely. (In a strong magnetic field, the spin degeneracy is lifted due to the Zeeman splitting which we are assuming to be very large.) Note that the δ -function singular DOS would imply rather singular thermodynamic properties of a 2DEG in the presence of an external magnetic field.

The above rather simple-minded and well-known¹ theoretical picture for a 2DEG in the presence of an external magnetic field does not hold for real 2DEG systems where all indications are that the DOS is a smooth function of energy (and, E_F certainly moves continuously through the Landau levels as quantum Hall-effect experiments definitively demonstrate). The DOS of a real 2DEG, while being a weakly oscillatory function of energy, does not have strong δ function singularities given by the non-interacting theory. For example, measured thermodynamic properties of a 2DEG in the presence of a strong external magnetic field such as the magnetic susceptibility² and the specific heat^{3,4} are rather weak oscillatory functions of B (or, N_s) implying a smooth (and small) variation in $D(E_F)$ as a function of E_F . Model calculations based on experimentally measured specific-heat or magnetic susceptibility show the DOS to be much smoother and broader than one would intuitively expect.²⁻⁴

In real systems, one expects disorder arising from random impurities in the system to have a smoothing effect on the singular $D(E)$ given by Eq. (1.5). In particular, scattering by the random impurities should broaden the DOS $D(E)$ with a characteristic broadening parameter $\Gamma_N(E)$ determined by the strength of the impurity-scattering potential associated with the random disorder. In the weak disorder case, one expects the standard ensemble-averaged diagrammatic perturbation theory to be valid in calculating the broadened DOS. Such a calculation was carried out a long time ago by Ando and Uemura¹ for a model of randomly distributed "short-range" (actually, zero-range) scatterers, neglecting the coupling between Landau levels. Within the self-consistent Born approximation (SCBA) and assuming that the scattering potential associated with the electron-impurity interaction is a pointlike δ function in real space, Ando and Uemura¹ obtained the following expression for the DOS in the strong-field limit:

$$D(E) = (2\pi l^2)^{-1} \sum_{N=0} (\pi\Gamma)^{-1} \left[1 - \left[\frac{E - E_N}{\Gamma} \right]^2 \right]^{1/2}, \quad (1.6)$$

where the constant level broadening Γ which, in this short-range approximation, is independent of the Landau-level index N (and energy E) depends only on the strength of the impurity-scattering potential and is, therefore, completely determined by the *zero-field* electronic mobility (μ_0) of the system:

$$\Gamma = (2\omega_c / \pi\tau)^{1/2} \equiv \Gamma_{SR}, \quad (1.7)$$

where the scattering time τ is extracted from the mobility (μ_0) of the system at zero magnetic field,

$$\tau = m\mu_0 / e. \quad (1.8)$$

We shall refer to the results (1.6)–(1.8) as the short-range approximation¹ [denoted by the subscript SR in Γ_{SR} given in Eq. (1.7)]. The approximations made in deriving these equations are many. (1) Weak disorder, so that SCBA involving only single impurity scattering is adequate; (2) the strong-field limit so that there is no coupling between Landau levels which implies that one must have $\omega_c \gg \Gamma$ with the overlap between Landau levels negligibly small; (3) zero-range electron-impurity interaction which can be characterized by a δ -function point scattering potential in real space.

The work presented in this paper goes beyond the above set of approximations and develops a more realistic theory of strong-field DOS in a 2DEG. [The Feynman diagrams for our theory are shown in Figs. 1(a)–1(d).] In particular, we relax approximations (2) and (3) listed above while still maintaining (1). Thus, we work within the SCBA assuming the impurity disorder to be weak so that the single-site scattering approximation [Figs. 1(a) and 1(b)] is adequate. But we take into account the fact that the impurities in a real 2DEG are *not* point δ -function scatterers—they are actually charged impurities which interact with an electron via the (screened) long-range Coulomb interaction [Figs. 1(c) and 1(d)]. We also include Landau-level coupling in our theory so that the strong-field ($\omega_c \gg \Gamma$) restriction is relaxed. Short versions of our theory for the DOS and of its application in calculating the thermodynamic properties of the 2DEG have earlier been reported by us.^{5,6} In this paper we provide the theoretical details and more complete numerical results for the DOS and the thermodynamic properties.

At first sight it seems that the approximations involved in the short-range theory of Ando and Uemura are quite reasonable and should be well valid in a high-mobility 2DEG at least in the limit of strong magnetic fields. One could invoke screening to assert that the *bare* long-range electron-impurity Coulomb interaction will be screened by the electrons to a short-range interaction for which the δ -function point scattering potential approximation may not be bad. One also expects high-mobility structures to have low collisional broadening so that the high-field approximation $\omega_c \gg \Gamma$ should be applicable for a fairly wide range of magnetic field and disorder strength. It turns out that these "intuitive" expectations are misleading and the situation is more subtle than suggested by this simple scenario.

The first thing to note is that the zero-field mobility is *not* always a good parameter to characterize the strength

of the disorder as is necessarily implied by the short-range approximation. In the short-range approximation the impurity potential is isotropic and there is only one scattering time (τ) in the problem at zero magnetic field which is both the transport relaxation time (τ) and the single-particle lifetime (τ_s). For a general finite range potential these two times could be very different⁷ with $\tau_{t,s}$

given by (at $T=0$ and in the leading order in impurity density)

$$\tau_{t,s}^{-1} = \frac{2\pi m}{\hbar^3} N_i \int \frac{d^2k}{(2\pi)^2} f_{t,s}(\theta) \left| u \left[2k_F \sin \frac{\theta}{2} \right] \right|^2 \times \frac{\delta(k - k_F)}{k} e^{-4k_F a \sin(\theta/2)}, \quad (1.9)$$

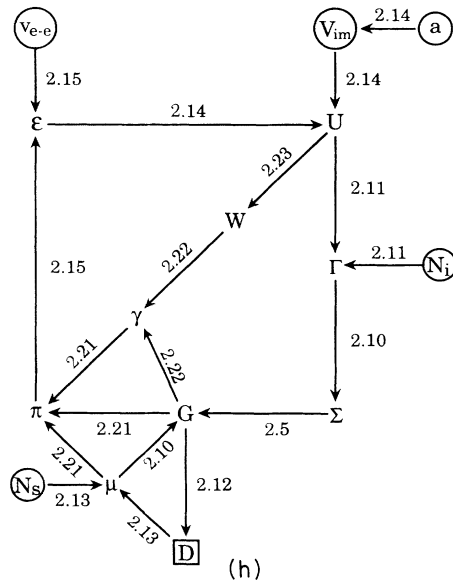
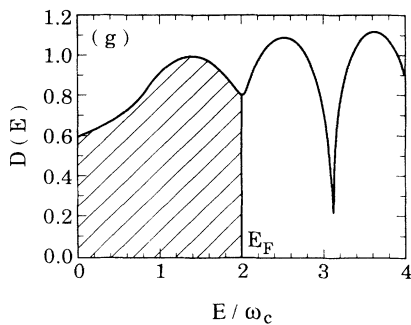
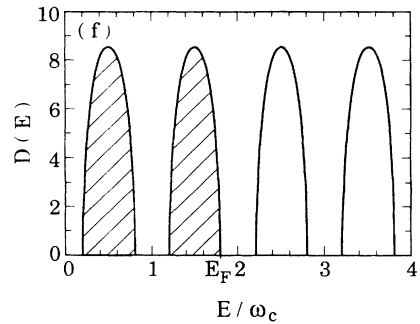
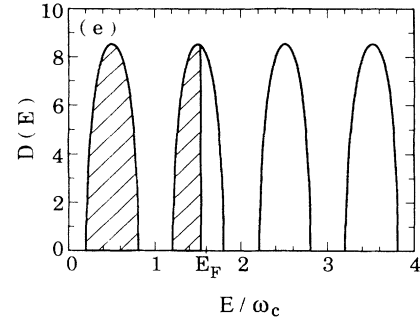
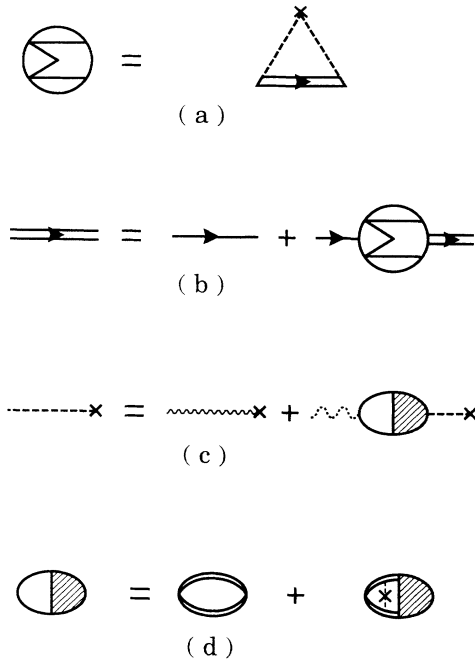


FIG. 1. (a)–(d) Show the Feynman diagrams used in our theory for the electron-impurity scattering [(a) and (b)] and screening [(c) and (d)], respectively. In (e)–(g) we show the qualitative dependence of the theory on the Fermi-level (E_F) location: In 1(e), E_F is located at the middle of a Landau level which is a metal-like situation and the system screens strongly; in 1(f) E_F is located in the gap making the system insulatorlike and, consequently, screening is weak; in 1(g) the situation is intermediate due to the Landau-level overlap. In 1(h) we show the nonlinear, self-consistent screening scheme with the corresponding equations from the text shown explicitly.

where $u(k)$ is the Fourier transform of the screened electron-impurity interaction, k_F is the 2D Fermi wave vector, N_i is the 2D real density of the randomly distributed impurity centers, and a is the distance between the plane of confinement of the 2DEG and the charged impurity centers (when they are distributed in the same 2D plane, $a=0$). The function $f(\theta)$ is given by

$$\begin{aligned} f_t(\theta) &= 1 - \cos\theta, \\ f_s(\theta) &= 1. \end{aligned} \quad (1.10)$$

Note that in Eq. (1.9) we assume that the electrons and the charged impurities are distributed in strict 2D planes which are separated by a distance a in the third direction (of course, a could be zero). In principle, one could consider a more complicated (three-dimensional) spatial impurity and electron distributions and Eq. (1.9) will then be appropriately modified by form factors associated with the confining electron wave function (in the z direction) and the impurity distribution function. The basic issue of the difference between τ_t and τ_s being discussed here is unaffected by these form-factor modifications.

It is clear from Eq. (1.9) that for a point δ function impurity scattering potential $\tau_t \equiv \tau_s$, and one has only a single relaxation time characterizing both transport and single-particle damping.⁷ [Mathematically, this is simply because the integral over the $\cos\theta$ factor vanishes for an isotropic potential $u(k)$ which becomes a constant in wave-vector space.] For a strongly screened short-range electron-impurity scattering potential the difference between τ_t and τ_s is small with τ_t (which is insensitive to forward scattering) being somewhat larger than τ_s . This, for example, is the situation in silicon inversion layers where screening is strong, and the electrons and the charged impurities reside very close to each other. In a modulation-doped high-mobility GaAs heterostructure, on the other hand, screening is weak and also, because of modulation doping, most of the scattering is forward scattering due to the long-range nature of the Coulomb interaction between the electrons and the charged impurities which are a distance a apart from each other. Depending on the values of a and N_i , τ_t can be orders of magnitudes larger than τ_s in high-mobility GaAs systems.⁷ Since τ_t determines mobility and τ_s determines the single-particle level broadening, it is clear that, even at zero magnetic field, there could be substantial errors in characterizing the single-particle level broadening by mobility.

This discrepancy between τ_t and τ_s is further exacerbated by the presence of a strong magnetic field where the concept of a single τ_s for *all* values of B (and/or N_s) does not apply (even for a constant N_i and a). In fact, it is easy to see that in a strong magnetic field scattering and screening must be obtained self-consistently where each determines (and is determined by) the other. The level broadening Γ is obviously determined by the (screened electron-impurity) scattering potential. But, electron screening itself is determined by the DOS which, in turn, is determined by Γ . Thus, screening and the scattering potential mutually determine each other and

must be obtained self-consistently. (The same, in principle, is true⁸ in an electron-impurity system without any external magnetic field, however, the effect is much weaker⁸ because the bare DOS is not singular.) One particularly spectacular aspect of this self-consistency is its strong intrinsic dependence on the position [Figs. 1(e)–1(g)] of the chemical potential E_F . For example, when E_F is at the middle [Fig. 1(e)] of a broadened Landau level, $E_F \approx (N + \frac{1}{2})\hbar\omega_c$, the system is like a “metal” because there are empty available electronic states at E_F for the electrons to make transitions to. This system obviously screens very strongly, making the effective electron-impurity interaction weak and short ranged, giving rise to small Γ . On the other hand, when E_F is near the edges [Fig. 1(f)] of a Landau level (and the magnetic field is large enough so that there is an energy gap in the DOS between the neighboring levels), the system is like an “insulator” with no free electronic states available infinitesimally above the Fermi level.

Screening is, consequently, weak and the effective electron-impurity interaction is long ranged and strong, giving rise to a large Γ . Thus, $\Gamma(E_F)$ (and therefore the DOS and screening) show strong oscillatory behavior as a function of the Fermi-level position. There have been many experimental verifications^{8–11} of this oscillatory behavior of level broadening, DOS, and screening as a function of E_F in a 2DEG under a strong external magnetic field. Clearly, self-consistency plays a strong role in this oscillatory behavior. In real systems, any possible Landau-level overlap [Fig. 1(g)] substantially modifies the screening and the nonlinear screening-scattering self-consistently becomes more complicated in the presence of Landau-level overlap.

We should emphasize that the self-consistent screening effect makes the short-range impurity scattering model a bad approximation in the strong-field situation. While the impurity potential is short ranged when the Fermi level is at the center of the Landau level, it is long ranged when the Fermi level lies at the Landau-level edges. This suggests that the disorder, in the presence of a magnetic field, cannot be characterized by the zero-field mobility. In fact, the qualitative discussion given above indicates that the strong-field broadening should, in general, be larger than the corresponding short-range result. This is precisely the experimental observation—thermodynamic measurements using three different kinds of experimental techniques, namely, the de Haas–van Alphen magnetization studies,² the specific heat⁴ and the magnetocapacitance measurements⁹ all indicate the DOS to be much broader than the short-range result. The general experimental consensus has been that the strong-field DOS of a 2DEG is, in general, much broader and flatter than that implied by the short-range SCBA-based scattering theoretic model with substantially more (than that given by the short-range theory) DOS in between the Landau levels. Transport measurements¹⁰ lend additional indirect support to the idea that the DOS is broader than the short-range result. Indirect evidence for oscillatory level-broadening and screening also comes from various optical experiments.¹¹

In this paper, we develop in detail the self-consistent

screening and level-broadening idea to calculate the electronic DOS of a 2DEG in the presence of a strong external magnetic field. We obtain our results as a function of the magnetic field and electron density for various values of the impurity density and spacer thickness (i.e., the distance separating the electron plane from the impurity plane). We also give results of our calculated specific heat and magnetization using the self-consistent DOS theory. The rest of the paper is organized as follows: In Sec. II we give the details of our theory with the relevant formula and equations; in Sec. III we present numerical results and provide a discussion of these results; and, finally we conclude in Sec. IV with a summary of our results and with a discussion of possible future directions. We should mention that there have been earlier attempts¹² at the self-consistent screening theory of strong-field level broadening along the same line being discussed here, but these attempts did not include actual calculations of the complete DOS and left out the Landau-level coupling effect.

II. THEORY

A. The density of states

We consider two-dimensional electrons interacting with the impurities (via the bare impurity scattering potential V_{im}) in an external magnetic field that is perpendicular to the xy plane in which the electrons are confined. We assume that the potential well in the z direction is deep and narrow enough so that the electrons occupy only the lowest subband in the z direction. Under the effective-mass approximation the Hamiltonian of the system can be written as

$$H = \sum_i^{N_e} \left[\frac{1}{2m^*} \left(\mathbf{p}_i + \frac{e}{c} \mathbf{A}_i \right)^2 + \sum_\alpha^{N_i} V_{\text{im}}(\mathbf{r}_i - \mathbf{r}_{\alpha}, z_\alpha) \right] + \frac{1}{2} \sum_{i \neq j} \frac{e^2}{\kappa |\mathbf{r}_i - \mathbf{r}_j|}, \quad (2.1)$$

where m^* is the band effective mass of the electron and κ the static dielectric constant of the background lattice. In a GaAs heterostructure m^* is $0.067m_e$, κ is 12.8. We consider scattering only by ionized charged impurities. In that case, the bare impurity-electron interaction potential V_{im} is Coulombic. \mathbf{A}_j is the vector potential associated with the external magnetic field. The main contribution of the electron-electron interaction in our model is the screening of the bare impurity-electron interaction. If we neglect other effects of electron-electron interac-

tion, we can work with the following effective single-electron Hamiltonian where the last term in Eq. (2.1) is suppressed and the second term is replaced by a statically screened electron-impurity interaction:

$$H_{\text{eff}} = \frac{1}{2m^*} \left(\mathbf{p} + \frac{e}{c} \mathbf{A} \right)^2 + \sum_\alpha^{N_i} u(\mathbf{r} - \mathbf{r}_\alpha, z_\alpha) \equiv H_0 + H_1. \quad (2.2)$$

The total Hamiltonian for the system is just the sum of H_{eff} over all the electrons. Here $u(\mathbf{r} - \mathbf{r}_\alpha, z_\alpha)$ is the screened impurity-electron interaction which has to be calculated self-consistently. For the sake of simplicity, we assume that the charged impurities are randomly distributed in a plane which is separated by a distance a from the 2D electron plane. Thus, our model is that of an electron plane of two-dimensional density N_s separated by a distance a from a charged impurity plane of impurity density N_i (we assume, as usual, that the impurity distribution is random). The separation allows us to simulate modulation doping in a simple manner by using the single parameter a . It is easy to generalize our calculation to the case where the impurities are distributed according to a certain distribution $P(z_\alpha)$ in the z direction and, the electron layer has a finite width also. In our case $P(z_\alpha)$ is $\delta(z_\alpha - a)$. As we have mentioned before, the zero-field mobility is not sufficient in correctly describing the DOS and the thermodynamic properties of a real experimental system as is assumed by the short-range interaction model. From the Hamiltonian of Eqs. (2.1) and (2.2), we need the following important physical parameters to describe the system: The electron density N_s , the impurity density N_i , the impurity charge $Z_i e$, the separation a , and the external magnetic field B . We keep $Z_i = 1$ and neglect the spin splitting throughout to minimize the number of parameters in the calculation. We choose the asymmetric Landau gauge $\mathbf{A} = (0, Bx, 0)$ for the magnetic field. The eigenfunction of H_0 is then given by

$$\Psi_{Np}(\mathbf{r}) = \frac{1}{L^{1/2}} e^{ipy} \chi_N(x - pl^2), \quad (2.3a)$$

with

$$\chi_N(x) = (2^N N! \pi^{1/2} l)^{-1/2} \exp \left[-\frac{x^2}{2l^2} \right] H_N \left[\frac{x}{l} \right], \quad (2.3b)$$

where N, p are, respectively, the Landau-level index and the free wave vector in the y direction. $H_N(x)$ is Hermite's polynomial and l is the magnetic length. The Hamiltonian can be written in the second quantization language as

$$H_{\text{eff}} = \sum_{N,p} E_N a_{Np}^\dagger a_{Np} + \sum_{N,p,N',p'} \langle Np | \sum_\alpha^{N_i} u(\mathbf{r} - \mathbf{r}_\alpha, a) | N'p' \rangle a_{Np}^\dagger a_{N'p'}. \quad (2.4)$$

We assume the density of impurities N_i to be low enough so that the SCBA involving only single impurity scattering [Fig. 1(a)] is adequate. Under this assumption, all localization effect has been neglected and the retarded Green's function $G_N^\dagger(E)$ and the self-energy $\Sigma_N^\dagger(E)$ for the N th Landau level can be determined by the Dyson's equation [Fig. 1(b)] as represented by the Feynmann diagram of Figs. 1(a) and 1(b):

$$G_N^\dagger(E) = [E - E_N - \Sigma_N^\dagger(E)]^{-1}, \quad (2.5)$$

$$\Sigma_N^\dagger(E) = \sum_{N', p'} u_{Np, N'p'} G_{N'}^\dagger(E) u_{N'p', Np}, \quad (2.6)$$

where

$$u_{Np, N'p'} = \langle Np | \sum_{\alpha} u(\mathbf{r} - \mathbf{r}_{\alpha}, a) | N'p' \rangle = \sum_{\alpha} \int d^2\mathbf{q} \exp(-i\mathbf{q} \cdot \mathbf{r}_{\alpha}) u(\mathbf{q}) \langle Np | \exp(i\mathbf{q} \cdot \mathbf{r}) | N'p' \rangle. \quad (2.7)$$

After some algebra, we get,

$$\langle Np | \exp(i\mathbf{q} \cdot \mathbf{r}) | N'p' \rangle = \delta(q_y - p + p') J_{NN'}(ql) \exp \left\{ i \left[q_x l (pl + p'l) / 2 + (n - m) \left[\varphi + \frac{\pi}{2} \right] \right] \right\}, \quad (2.8)$$

where

$$q = (q_x^2 + q_y^2)^{1/2}, \quad \varphi = \arctg[q_y / q_x] \text{sign}(N - N')$$

and

$$J_{NN'}(ql) = (m! / n!)^{1/2} \exp(-q^2 l^2 / 4) \times (ql / 2^{1/2})^n = {}_m L_m^{n-m}(q^2 l^2 / 2) \quad (2.9)$$

with $n = \max(N, N')$, $m = \min(N, N')$, and $L_m^{n-m}(x)$ is the associated Laguerre polynomial. Using the fact that $u_{Np, N'p'}$ and $u_{N'p', Np}$ interact with the same impurity [cf. Fig. 1(a)] and using Eq. (2.7), (2.8), and (2.5), Eq. (2.6) can be written as

$$\begin{aligned} \Sigma_N^\dagger(E) &= N_i \sum_{N'} \frac{1}{(2\pi)^2} \int d^2\mathbf{q} |u(\mathbf{q})|^2 J_{NN'}^2(ql) G_{N'}^\dagger(E) \\ &= \sum_{N'} \frac{1}{4} \Gamma_{NN'}^2 [E - E_{N'} - \Sigma_{N'}^\dagger(E)]^{-1} \end{aligned} \quad (2.10)$$

with

$$\frac{1}{4} \Gamma_{NN'}^2 = N_i \frac{1}{(2\pi)^2} \int d^2\mathbf{q} |u(\mathbf{q})|^2 J_{NN'}^2(ql) \quad (2.11)$$

which is the coupling between different Landau levels and is related to the broadening of the various Landau levels. If we know $\Gamma_{NN'}$, we are able to calculate $\Sigma_N^\dagger(E)$ by solving Eq. (2.10). Once $\Sigma_N^\dagger(E)$ is known, one can get the Green's function $G_N^\dagger(E)$ according to Eq. (2.5) and the density of states which is proportional to the imaginary part of Green's function:

$$D(E) = \sum_N D_N(E) = -(g_s / 2\pi^2 l^2) \sum_N \text{Im} G_N^\dagger(E), \quad (2.12)$$

where g_s is the spin degeneracy. The Fermi energy is determined by the 2D density of electrons,

$$\int_0^{E_F} D(E) dE = N_s. \quad (2.13)$$

The screened electron-impurity interaction within the random-phase approximation (RPA) is given by [cf. Fig. 1(c)],

$$u(\mathbf{q}) = V_{\text{im}}(\mathbf{q}) / \epsilon(q) \quad (2.14)$$

with

$$V_{\text{im}}(q) = \frac{2\pi e^2}{\kappa q} e^{-iqa}, \quad (2.14a)$$

as the Fourier transform of 2D electron-impurity interaction (κ is the background dielectric constant), and

$$\epsilon(q) = 1 - v_{e-e}(q) \Pi(q), \quad (2.15)$$

where

$$v_{e-e}(q) = \frac{2\pi e^2}{\kappa q}, \quad (2.15a)$$

is the Coulomb interaction. Here $\Pi(q) = \Pi(\mathbf{q}, \omega = 0)$ is the irreducible static electronic polarizability function and v_{e-e} is the Coulomb interaction. Notice that we must distinguish electron-impurity interaction and electron-electron interaction, because although both of them are, in principle, Coulombic, the electrons and the impurities are in two spatially separated planes. We also want to point out that because of the external magnetic field, the electron Green's function is not translationally invariant but $\Pi(\mathbf{r}_1, \mathbf{r}_2)$ is still translationally invariant. We can, therefore, still use the Fourier representation in Eqs. (2.7)–(2.11). We retain the vertex correction (consistent with the SCBA) in our calculation of the polarizability $\Pi(\mathbf{q}, \omega)$ by keeping all the electron-impurity ladder diagrams as shown in the Feynman diagram of Fig. 1(d). Using Matsubara finite-temperature Green's function,

$$\Pi(\mathbf{q}, i\omega) = -\frac{2}{\beta} \sum_{ip_n} \sum_{N, p} \sum_{N', p'} G_N(ip_n + i\omega) G_{N'}(ip_n) \delta(-q_y + p - p') M_{NN'}(\mathbf{q}) \gamma_{Np, N'p'}(ip_n + i\omega, ip_n, \mathbf{q}) \quad (2.16)$$

with

$$M_{NN'}(\mathbf{q}) = (m! 2^m / n! 2^n)^{1/2} \exp(-q^2 l^2 / 4) (q_y l + i q_x l)^{n-m} L_m^{n-m}(q^2 l^2 / 2). \quad (2.17)$$

Here again $n = \max(N, N')$ and $m = \min(N, N')$. We do the frequency summation of Eq. (2.17) in the complex plane taking into account the branch cuts. For the static screening case ($\omega \rightarrow 0$), we get

$$\begin{aligned} S &\equiv \frac{1}{\beta} \sum_{ip_n} G_N(ip_n + i\omega) G_{N'}(ip_n) \gamma_{NP, N'p'}(ip_n + i\omega, ip_n, \mathbf{q}) \\ &= -\frac{1}{\pi} \int dE n_F(E) \text{Im}[G_N(E + i0) G_{N'}(E + i0) \gamma_{NN'}(E, \mathbf{q})], \end{aligned} \quad (2.18)$$

where $n_F(E)$ is the Fermi distribution function. We assume that $\gamma_{NN'}(E, \mathbf{q})$ is a continuous function on the branch cuts. $\gamma_{NN'}$ is determined by the following self-consistent equation:

$$\gamma_{NN'}(E, \mathbf{q}) = M_{NN'}^*(\mathbf{q}) + \sum_{L, L'} W(N, N', L, L'; \mathbf{q}) G_L^\dagger(E) G_{L'}^\dagger(E) \gamma_{LL'}(E, \mathbf{q}), \quad (2.19)$$

where $M_{NN'}^*(\mathbf{q})$ is the complex conjugate of $M_{NN'}(\mathbf{q})$ and $W(N, N', L, L'; \mathbf{q})$ is given by

$$W(N, N', L, L'; \mathbf{q}) = \frac{1}{(2\pi)^2} \int d^2\mathbf{p} \exp(i|\mathbf{q} \times \mathbf{p}|l^2) |u(\mathbf{p})|^2 (p_y l + ip_x l)^{N-N'} (p_y l - ip_x l)^{L-L'} J_{NL}(pl) J_{N'L'}(pl). \quad (2.20)$$

Finally, using (2.18)–(2.20) in Eq. (2.16), we get,

$$\Pi(\mathbf{q}) = -\frac{1}{\pi} \int dE n_F(E) \Pi^\dagger(\mathbf{q}, E) \quad (2.21a)$$

$$\Pi^\dagger(\mathbf{q}, E) = (\pi l^2)^{-1} \sum_{N, N'} M_{NN'}(\mathbf{q}) \text{Im}[G_N^\dagger(E) G_{N'}^\dagger(E) \gamma_{NN'}(E, \mathbf{q})]. \quad (2.21b)$$

We have now closed the self-consistency loop [Fig. 1(h)] for our calculation. If we start with a initial guess of, say the dielectric function $\epsilon(q)$, then from (2.15) we know the screened electron-impurity interaction $u(q)$. From $u(q)$ we can calculate the self-energy $\Sigma_N^\dagger(E)$ according to Eqs. (2.10) and (2.11). We can then get the retarded Green's function, the density of states, and the Fermi energy from Eqs. (2.5), (2.12), and (2.13), respectively. Using the quantities so obtained, we can go back and calculate $\Pi(q)$ and $\epsilon(q)$ from Eqs. (2.21) and (2.15), respectively. We keep doing this until all the physical quantities of interest become convergent. The self-consistency loop is shown in Fig. 1(h).

To simplify the self-consistent calculation, we ignore the Landau-level coupling effect in the vertex correction. Equations (2.19) and (2.20) can then be written as

$$\gamma_{NN'}(E, \mathbf{q}) = \delta_{NN'} M_{NN'}^*(\mathbf{q}) [1 - W(N, \mathbf{q}) G_N^\dagger(E) G_N^\dagger(E)]^{-1}, \quad (2.22)$$

here $\delta'_{N,N}$ is a Kornecker δ function and

$$\begin{aligned} W(N, q) &= W(N, N, N, N; \mathbf{q}) \\ &= \frac{1}{2\pi} \int_0^\infty p dp |u(\mathbf{p})|^2 J_{NN}^2(pl) J_0(qpl^2) \end{aligned} \quad (2.23)$$

in which $J_0(x)$ is the zeroth-order Bessel function.

In Fig. 1(h) we show the self-consistent loop for our calculation whereas Figs. 1(a)–1(d) show the Feynman diagrams used in the calculation. A starting guess for the dielectric function could be, for example, the corresponding zero-field Thomas-Fermi result. We demand our calculated self-consistent quantities (e.g., D, E_F) to converge within 0.5% and typically, this requires 50–500 iterations of our self-consistent loop. Simpler theoretical approximations¹² to various parts of this self-consistent scheme have earlier been discussed in the literature. In

the next section we discuss how this self-consistent DOS can be applied to calculate thermodynamic properties of the 2DEG.

B. The thermodynamic properties

We have calculated the DOS at zero temperature. In calculating thermodynamic properties we assume that we can neglect any explicit temperature dependence of the DOS (arising, for example, from the temperature dependence of screening and/or the chemical potential) which is a reasonable assumption because we are interested only in a rather low-temperature regime (0–10 K) where the temperature dependence of the DOS is exponentially small.

The free energy and the two-dimensional density of electrons of the system are given by

$$F = \int_{-\infty}^{\infty} dE n_F(E) E D(E), \quad (2.24)$$

$$N_s = \int_{-\infty}^{\infty} dE n_F(E) D(E), \quad (2.25)$$

respectively. Here $n_F(E) = \{\exp[\beta(E - \mu)] + 1\}^{-1}$, $\beta = (k_B T)^{-1}$, and μ is the chemical potential. In the experimental systems N_s is fixed and does not depend on the temperature. Taking the derivative with respect to temperature of both Eqs. (2.24) and (2.25) we get for the specific heat C_v of the 2DEG:

$$C_v = \int_{-\infty}^{\infty} \frac{dn_F(E)}{dT} (E - \mu) D(E) dE \quad (2.26)$$

with

$$\frac{dn_F(E)}{dT} = \frac{\beta e^{\beta(E - \mu)}}{(e^{\beta(E - \mu)} + 1)^2} \left[\frac{E - \mu}{T} + \frac{d\mu}{dT} \right]. \quad (2.27)$$

$d\mu/dT$ can be calculated from Eq. (2.25),

$$\frac{d\mu}{dT} = -\frac{1}{T} \frac{\int_{-\infty}^{\infty} A(E, \beta)(E - \mu)D(E)dE}{\int_{-\infty}^{\infty} A(E, \beta)D(E)dE} \quad (2.28a)$$

in which

$$A(E, \beta) = \frac{\beta e^{\beta(E - \mu)}}{[e^{\beta(E - \mu)} + 1]^2}. \quad (2.28b)$$

Combining Eqs. (2.26), (2.27), and (2.28) we get

$$C_V = \frac{1}{T} \int_{-\infty}^{\infty} A(E, \beta)(E - \mu)^2 D(E) dE - \frac{1}{T} \frac{[\int_{-\infty}^{\infty} A(E, \beta)(E - \mu)D(E)dE]^2}{\int_{-\infty}^{\infty} A(E, \beta)D(E)dE}. \quad (2.29)$$

The function $A(E, \beta)$ defined by Eq (2.28b) peaks around $E \approx \mu$ with a width of about $k_B T$. μ is self-consistently calculated from Eq. (2.25). In zero magnetic field and for $k_B T \ll \mu$, Eq. (2.29) can be expanded in a Sommerfeld expansion to give the simple and well-known result

$$C_V = \frac{\pi^2}{3} k_B^2 T D(E_F), \quad (2.30)$$

where $E_F = \mu(T=0)$ is the Fermi energy and we retain only the linear order term in temperature. We find that even at the low temperatures explored experimentally (1–10 K) a result like Eq. (2.30) is not valid for a 2DEG in a strong magnetic field. In fact, C_V has nonlinear dependence on T in the temperature range 1–10 K at a fixed magnetic field. We can show analytically that for $\omega_c \gg k_B T \gg \Gamma$ the specific heat varies as Γ^2/T^2 instead of the linear Fermi gas behavior of Eq. (2.30). (Here Γ is the Landau-level broadening.) We find that the actual behavior $C_V(T)$ depends sensitively on relative magnitudes of $k_B T$, μ , ω_c , and Γ . In particular, $C_V(T)$ can show very pronounced nonmonotonic behavior. It tells us that in the presence of an external magnetic field (and impurity-electron interaction), since we have two more relevant energy scales of the system, namely, the separation between Landau levels ω_c and the widths of each of them Γ_N , the simple linear temperature dependence of a Landau Fermi liquid does not hold in a 2DEG.

In a similar spirit, the orbital (or the Landau) magnetization of the system is given by (at $T=0$)

$$M = \int_{-\infty}^{-E_F} (E_F - E) \frac{\partial D(E)}{\partial B} dE. \quad (2.31)$$

Numerical calculation of M based on Eq. (2.31) is tricky because of the derivative term—instead we use a polynomial fit to the free energy as a function of B and evaluate M directly from the free energy. Thus our calculated M is not as accurate as our calculated C_V .

We discuss our calculated results for the DOS, C_V and M in the Sec. III.

III. RESULTS AND DISCUSSIONS

From our discussion in I and II it is clear that the self-consistent DOS of a 2DEG in the presence of an external

magnetic field is a complicated nonlinear function of a number of variables—in addition to depending on the magnetic field B , $D(E)$ depends on the 2D electron density N_s , the impurity density N_i , and the effective spacer thickness or the electron-impurity separation a (note that if we relax our δ -doping model for the charge impurities, the impurity configuration would have to be described by more variables). Thus, $D(E)$ in our theory is an explicit function of four variables B , N_s , and N_i , and a . The corresponding situation for the short-range theory [cf. Eqs. (1.6) and (1.7)] is simpler with N_s , N_i , and a entering the DOS only through the zero-field mobility μ_0 which is experimentally measured. The free-electron result is, of course, a series of δ functions located at the Landau energies, dependent only on the magnetic field. Since the short-range scattering result for the DOS is widely (in fact, almost exclusively) used, we will show our calculated self-consistent results along with the corresponding short-range results for the sake of comparison. As one would see, in many experimentally relevant situations the self-consistent DOS is strikingly different from the short-range result and, as emphasized in the Introduction, in general, the self-consistent DOS is broader and flatter than the short-range result, being in closer agreement with the measured DOS. All our results are calculated for a 2DEG confined in a GaAs heterostructure with the impurity plane separated by a distance a from the 2D electron plane.

In Fig. 2 we show our calculated self-consistent DOS, $D(E)$ with $a = 50 \text{ \AA}$, $\mu_0 = 80\,000 \text{ cm}^2/\text{Vs}$, and $N_s = 2 \times 10^{11} \text{ cm}^{-2}$ for three values of the magnetic field $B =$ (a) 2.6, (b) 3.4, and (c) 4.4 T. The self-consistent DOS is shown by the solid lines whereas the dashed lines give the short-range result and the Fermi level (i.e., the chemical potential) E_F is also shown. The self-consistent DOS is much broader than the short-range results, and for $B = 2.6 \text{ T}$ [Fig. 2(a)], where Landau-level overlap is very significant, the self-consistent DOS, in sharp contrast to the oscillatory short-range result, is almost flat, being qualitatively similar to the zero-field noninteracting two-dimensional density of states which is a constant. At higher fields [Figs. 2(b) and 2(c)], the self-consistent DOS shows much weaker oscillations as a function of E than does the short-range result.

In general, the zero-field mobility is not a good parameter in characterizing the strong-field DOS. This is most clearly seen from Fig. 3 where we depict the calculated self-consistent DOS for $\mu_0 = 400\,000 \text{ cm}^2/\text{Vs}$, $N_s = 2 \times 10^{11} \text{ cm}^{-2}$, $B = 3.4 \text{ T}$ with three different values of the electron-impurity separation $a = 0$ (dot-dashed line), 100 \AA (heavy dash), and 150 \AA (solid) and compare it with the short-range result (light dash) which is uniquely determined by the zero-field mobility. In varying the spacer thickness parameter a (while keeping μ_0 fixed) we obviously had to adjust the impurity concentration N_i appropriately. It is obvious from Fig. 3 that the self-consistent DOS is not uniquely determined by the zero-field mobility μ_0 , but is a function of both a and N_i (or, more generally, of the actual impurity distribution in the sample). We emphasize that each curve in Fig. 3 represents the calculated DOS of a 2DEG with identical

values of N_s and μ_0 , but with different impurity distributions (i.e., N_i and a in our model).

In Fig. 4 we show some more representative self-consistent DOS, $D(E)$, for a number of different values of B , N_s , μ_0 , and a . From these results (Figs. 2–4) and from many other sets of such results that we have (which are not being shown here), we form the following general conclusions about our calculated self-consistent DOS.

(1) In general, self-consistent $D(E)$ could be very different from the short-range result—in particular, self-

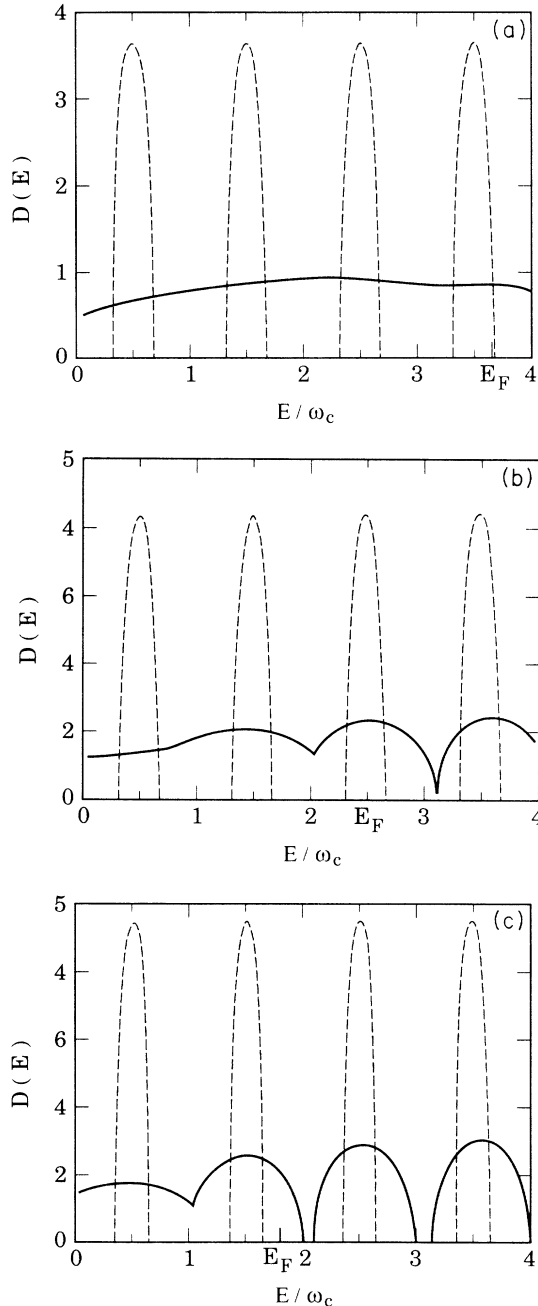


FIG. 2. The DOS $D(E)$ is shown with $a = 50 \text{ \AA}$, $\mu_0 = 80\,000 \text{ cm}^2/\text{Vs}$, $N_s = 2 \times 10^{11} \text{ cm}^{-2}$ for magnetic field values $B =$ (a) 2.6, (b) 3.4 T, and (c) 4.4. Dashed lines are the results for the short-range model.

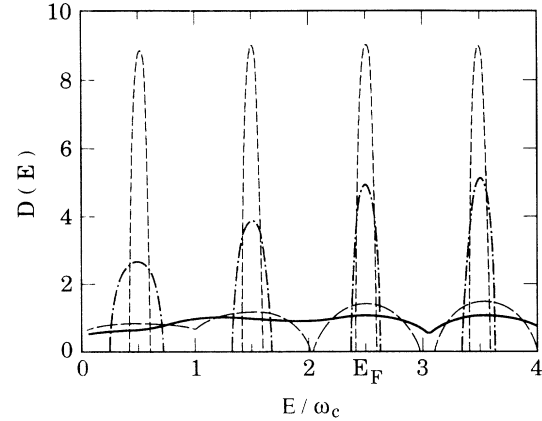


FIG. 3. The DOS $D(E)$ is shown with fixed $\mu_0 = 4\,000\,000 \text{ cm}^2/\text{Vs}$, $N_s = 2 \times 10^{11} \text{ cm}^{-2}$, and $B = 3.4 \text{ T}$, but with variable $a = 0$ (dot-dashed line), 100 \AA (short-dashed line), and 150 \AA (solid line). Short-range model results are shown by the long-dashed line.

consistent DOS is broader and flatter than the short-range result.

(2) The zero-field mobility μ_0 does not uniquely parametrize the self-consistent DOS which depends sensitively on the actual impurity distribution in a modulation-doped structure.

(3) For a fixed value of μ_0 , the self-consistent DOS gets closer to the short-range result as the spacer thickness a (or the effective electron-impurity separation) decreases (implying an increase of N_i).

(4) For a fixed value of the separation parameter a , the self-consistent DOS gets closer to the short-range result as the zero-field mobility μ_0 increases (implying a decrease of N_i).

(5) For a fixed value of the impurity density N_i , the self-consistent DOS gets closer to the short-range result as a decreases (implying a decrease of μ_0).

(6) In any given situation, self-consistent $D(E)$ becomes qualitatively similar to the short-range result for $E \gg E_F$.

(7) In general, the self-consistent DOS is qualitatively closer to the short-range result for higher fields.

(8) Finally, knowing $D(E)$ does not uniquely give $D(E_F) = D(E = E_F)$ because there is an implicit dependence of the DOS on the chemical potential (to be discussed below).

The above qualitative remarks about our calculated self-consistent DOS are all in agreement with the experimental conclusions from various thermodynamic (e.g., magnetization, capacitance, and specific heat), transport and optical measurements. We should point out (and this will be discussed later) that a direct comparison between our self-consistent theory and experimental results is difficult because one does not, in general, know the detailed impurity distribution in an experimental sample, and, as emphasized above, the self-consistent DOS depends sensitively on the details of the impurity distribution, rather than on the mobility μ_0 itself.

In Fig. 5 we show our calculated screening function for

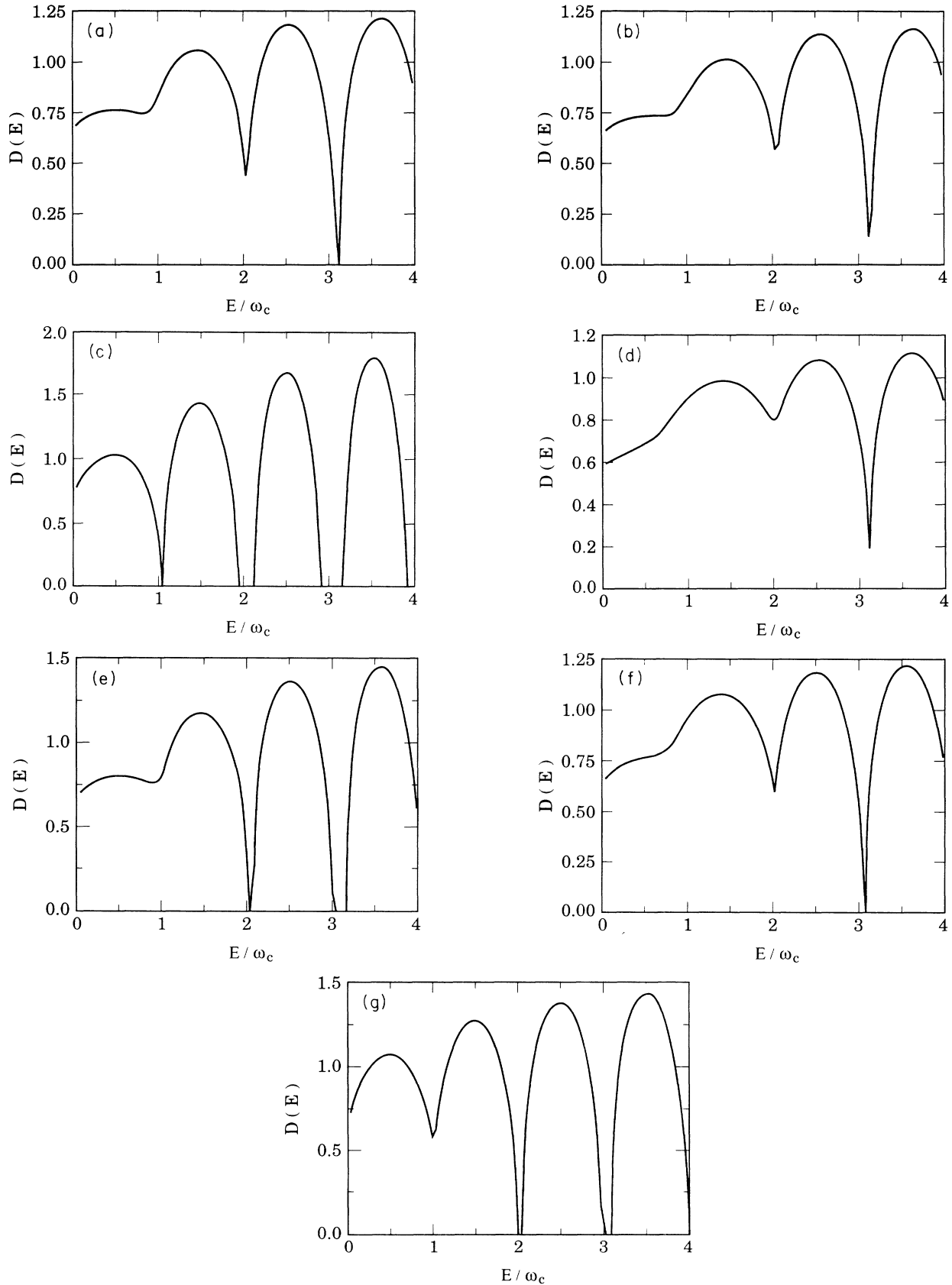


FIG. 4. The DOS $D(E)$ is shown for various parameters: (a) $a=0$ Å, $\mu_0=55000$ cm²/V s, $N_s=2 \times 10^{11}$ cm⁻², $B=4.0$ T, and $E_F=2.2038\omega_c$. (b) Same as (a) except $B=3.5$ T and $E_F=2.5393\omega_c$, (c) $a=50$ Å, $\mu_0=295000$ cm²/V s, $N_s=2 \times 10^{11}$ cm⁻², $B=3.5$ T, and $E_F=2.4397\omega_c$. (d) Same as (c) except $B=2.5$ T and $E_F=3.5867\omega_c$. (e) Same as (c) except $B=3.0$ T and $E_F=2.7517\omega_c$. (f) $a=50$ Å, $\mu_0=80000$ cm²/V s, $N_s=3 \times 10^{11}$ cm⁻², $B=5.7$ T, and $E_F=2.2454\omega_c$. (g) Same as (f) except $B=8.6$ T and $E_F=1.4500\omega_c$.

$B = 3.6$ T, $N_s = 2 \times 10^{11}$ cm $^{-2}$, $a = 0$, and $\mu_0 = 30\,000$ cm 2 /Vs—the static polarizability and the dielectric function are shown in Figs. 5(a) and 5(b), respectively, whereas in Fig. 5(c) we show the self-consistent DOS itself.

In comparison with experimental results one often needs the DOS at the Fermi energy (chemical potential), $D(E_F)$, rather than the full $D(E)$. Normally, as, for example, in the short-range model, $D(E_F)$ is uniquely

determined by $D(E)$, and is given by $D(E_F) \equiv D(E = E_F)$ from Eq. (1.6). But in the self-consistent model there is an implicit dependence of the DOS on the chemical potential (in addition to the explicit dependence through energy) because screening depends on where the Fermi level lies (i.e., whether E_F is at the middle of the Landau level leading to strong screening or whether it is at the edge of a Landau level leading to weak screening). Thus the self-consistent DOS, $D(E)$, is a function of E_F through the nonlinear screening, i.e., $D(E) \equiv D(E; E_F)$. This implicit dependence of the DOS on the actual position of the Fermi level is a novel feature of the screening-level-broadening self-consistency being studied here. In the short-range theory knowing $D(E)$ [cf. Eq. (1.6)] completely defines $D(E_F)$, but the same is *not true* in the self-consistent theory.

In Fig. 6(a) we show our calculated self-consistent $D(E_F) \equiv D(E = E_F; E_F)$ as a function of the applied magnetic field B for $N_s = 2 \times 10^{11}$ cm $^{-2}$; $\mu_0 = 30\,000$ cm 2 /Vs, and $a = 0$ Å. The self-consistent result is shown by the solid line whereas the short-range result [i.e., Eq. (1.6) with $E = E_F$] is shown as the dashed line. In Fig. 6(b) we show the calculated level broadening Γ_n for the individual Landau levels for the same as in Fig. 6(a). The short-

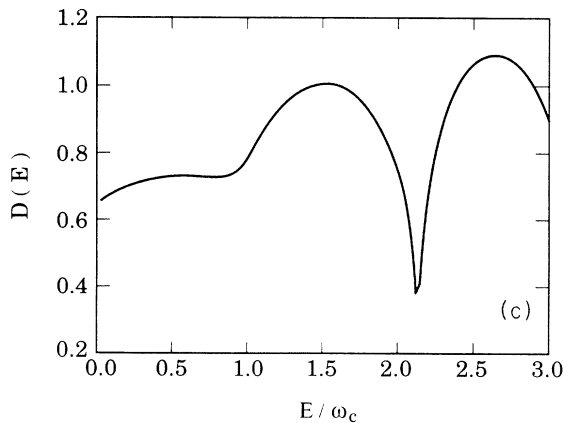
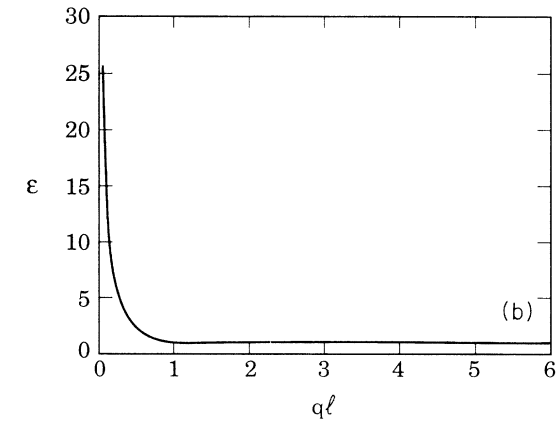
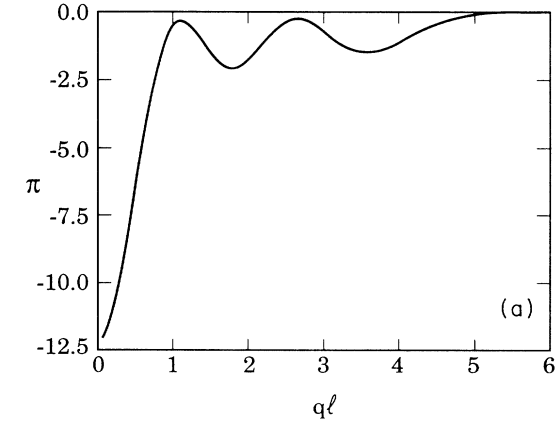


FIG. 5. (a) The polarizability function $\Pi(q)$, (b) the dielectric function $\epsilon(q)$ as a function of wave vector q for $a = 0$ Å, $\mu_0 = 30\,000$ cm 2 /Vs, $N_s = 2 \times 10^{11}$ cm $^{-2}$, and $B = 3.6$ T. (c) DOS $D(E)$ of the system.

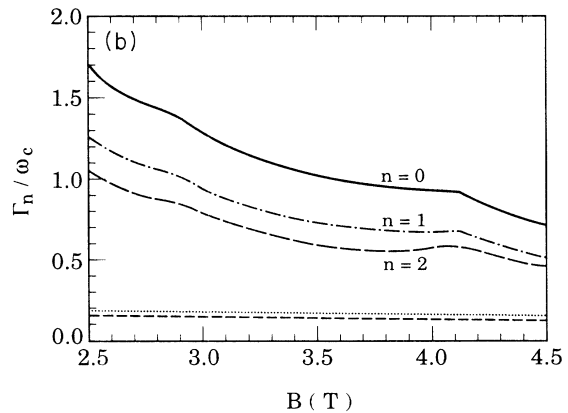
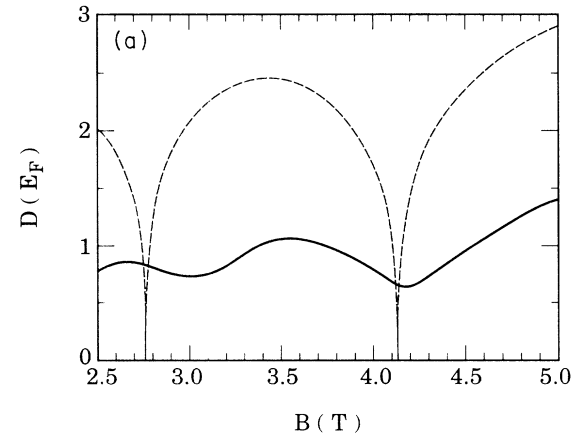


FIG. 6. (a) The DOS $D(E_F)$, and (b) the Landau-level broadening Γ_n , as a function of magnetic field for the system as in Fig. 5. The dashed line is the short-range-model (SRM) result. The dotted line in (b) is calculated from Eq. (1.7) using τ_s instead of τ_l .

range result for the Landau-level broadening Γ [given by Eq. (1.7)] which is independent of the Landau level index n is shown by the lowest dashed curve. We also show by the dotted line the short-range result using the zero-field single-particle broadening (rather than the mobility broadening) for comparison.

In Figs. 7(a) and 7(b) we show the same thing [i.e., $D(E_F)$ and Γ_n as a function of B] as in Figs. 6(a) and 6(b), but for $a = 50 \text{ \AA}$ and $\mu = 80\,000 \text{ cm}^2/\text{V s}$ with all the other parameters the same as in Fig. 6.

In Fig. 8 we show our calculated DOS [Fig. 8(a)] and level broadening [Fig. 8(b)] as a function of the electron density N_s for fixed values of $B = 4 \text{ T}$, $a = 0 \text{ \AA}$, $\mu_0 = 30\,000 \text{ cm}^2/\text{V s}$. In Fig. 8(a) the self-consistent and the short-range results are shown by the solid and the dashed lines, respectively, whereas in Fig. 8(b) the self-consistent results for various Landau levels are shown (the short-range Γ is a constant of value around $\Gamma/\omega_c \approx 0.1$).

Results shown in Figs. 6–8 clearly demonstrate the main qualitative features of the self-consistent DOS *vis-à-vis* the widely used short-range result. In general, the self-consistent broadening is substantially (by factors of 1.5–100) larger than the short-range broadening, and, consequently, the self-consistent DOS is substantially

flatter than the short-range DOS. For example, in Figs. 6–8 the relative variation (i.e., the difference between the peaks and the valleys) in the DOS is about 10–40 % in the self-consistent theory and is about 100–300 % in the short-range theory. Many experimental papers in the last ten years have concluded that in modulation-doped GaAs heterostructures the strong-field DOS is substantially flatter (and the broadening significantly larger) than the results of the short-range theory. We believe that the self-consistent screening theory of the DOS as developed in this paper is a possible explanation for this discrepancy.

Finally, in Fig. 9 we show the calculated self-consistent Landau-level broadening Γ_n for fixed values of $a = 50 \text{ \AA}$ and $N_s = 2 \times 10^{11} \text{ cm}^{-2}$ as a function of the impurity density N_i for two different values of the magnetic field: $B = 3.5 \text{ T}$ [Fig. 9(a)] and 4.2 T [Fig. 9(b)]. In the short-range theory, $\Gamma \propto N_i^{1/2}$ because the zero-field mobility μ_0 is inversely proportional to N_i (for fixed a and N_s) in the single-site approximation. In general, the self-consistent level broadening does not have a simple power-law dependence on the impurity density N_i because the self-consistent theory depends sensitively on a number of parameters such as E_F , a , N_s , and B . The dependence on N_i in Fig. 9 is, however, closer to a linear power law than a square root one.

The above representative results for the calculated

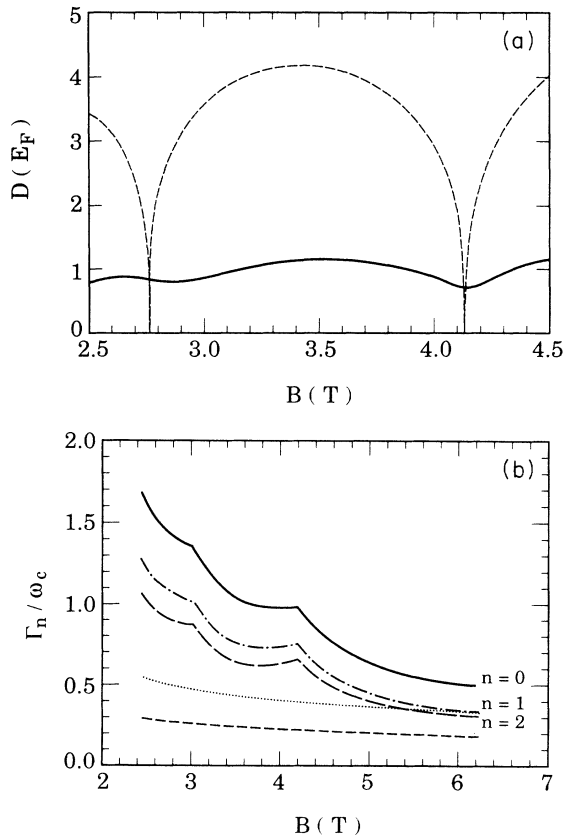


FIG. 7. (a) The DOS $D(E_F)$, and (b) the Landau-level broadening Γ_n as a function of magnetic field for $a = 50 \text{ \AA}$, $\mu_0 = 80\,000 \text{ cm}^2/\text{V s}$, and $N_s = 2 \times 10^{11} \text{ cm}^{-2}$. The dashed line is the SRM result. The dotted line in (b) is calculated from Eq. (1.7) using τ_s instead of τ_l .

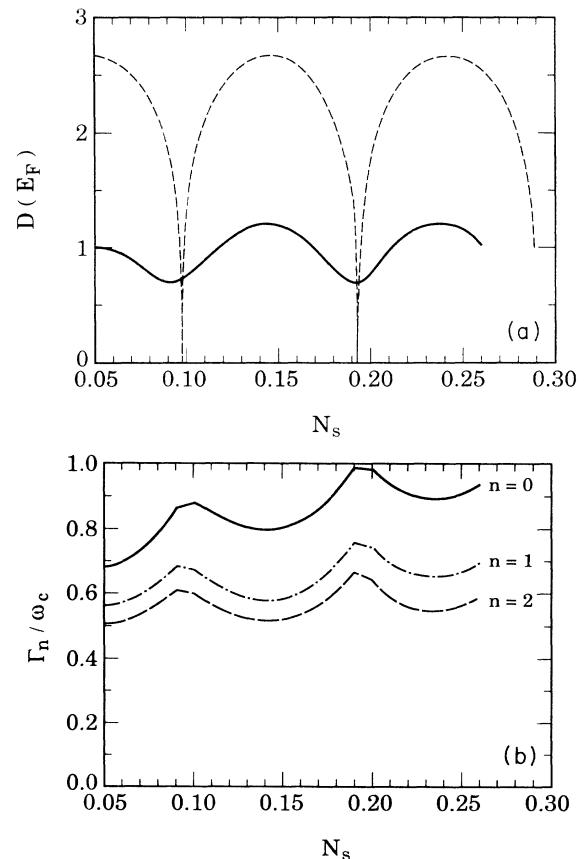


FIG. 8. (a) The DOS $D(E_F)$, and (b) the Landau-level broadening Γ_n , as a function of the electron density N_s .

DOS give one a good flavor of the qualitative features of the self-consistent theory. Obviously, there being a large number of parameters and variables in the problem (viz. N_s , N_i , a , μ_0 , E_F , B , n , E) a single paper, no matter how comprehensive, cannot really provide an exhaustive set of results for all possible experimental situations. We have, therefore, emphasized here generic features of the self-consistent DOS, emphasizing, in particular, its difference with the simple (and extensively used) short-range theory. The self-consistent theory is in much better agreement with the experiment results, not only quantitatively but also qualitatively. But, in some sense one pays a price for this experimental agreement—one cannot characterize the self-consistent DOS by a single suitable parameter in contrast to the short-range theory where zero-field mobility completely and uniquely defines the strong-field DOS. Thus, the simplicity of the short-range theory is lost and, in order to compare with experimental results, one must now know the actual impurity distribution and different impurity distributions having the same zero-field mobility may have strikingly different strong-field DOS (cf. Fig. 3). This dependence of the DOS and the level broadening on the details of the impurity distribution and the inadequacy of μ_0 as a unique parameter defining the strong-field DOS has been repeatedly discussed in the experimental literature.

Experimentally, the most direct information about the DOS comes from thermodynamic measurements such as

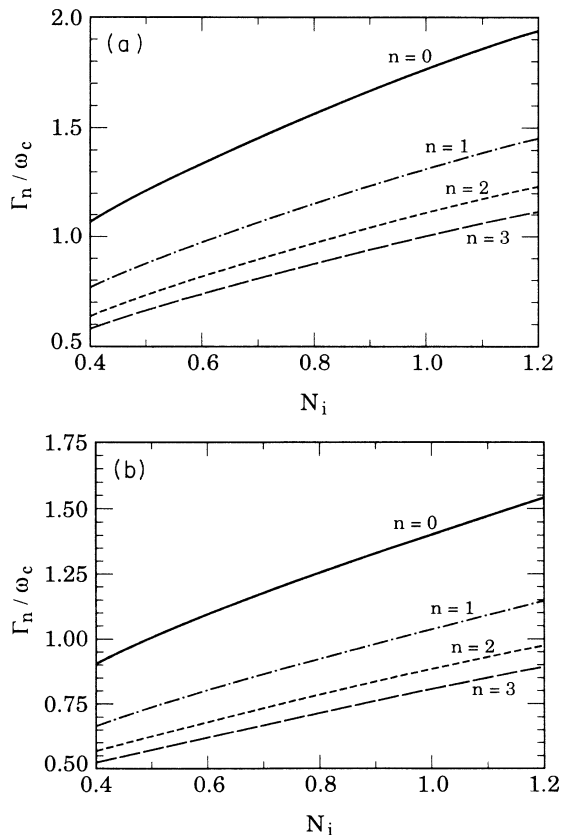


FIG. 9. The Landau-level broadening Γ_N as a function of the impurity density N_i at $B =$ (a) 3.5 T, and $B =$ (b) 4.2 T.

the electronic specific heat (C_v) and magnetization (M) which can be calculated (see II for details) once the self-consistent DOS is known. In Figs. 10–12 we show our calculated C_v and M of a 2DEG in the presence of an external magnetic field using the self-consistent DOS.

In Fig. 10 we show the calculated temperature dependence

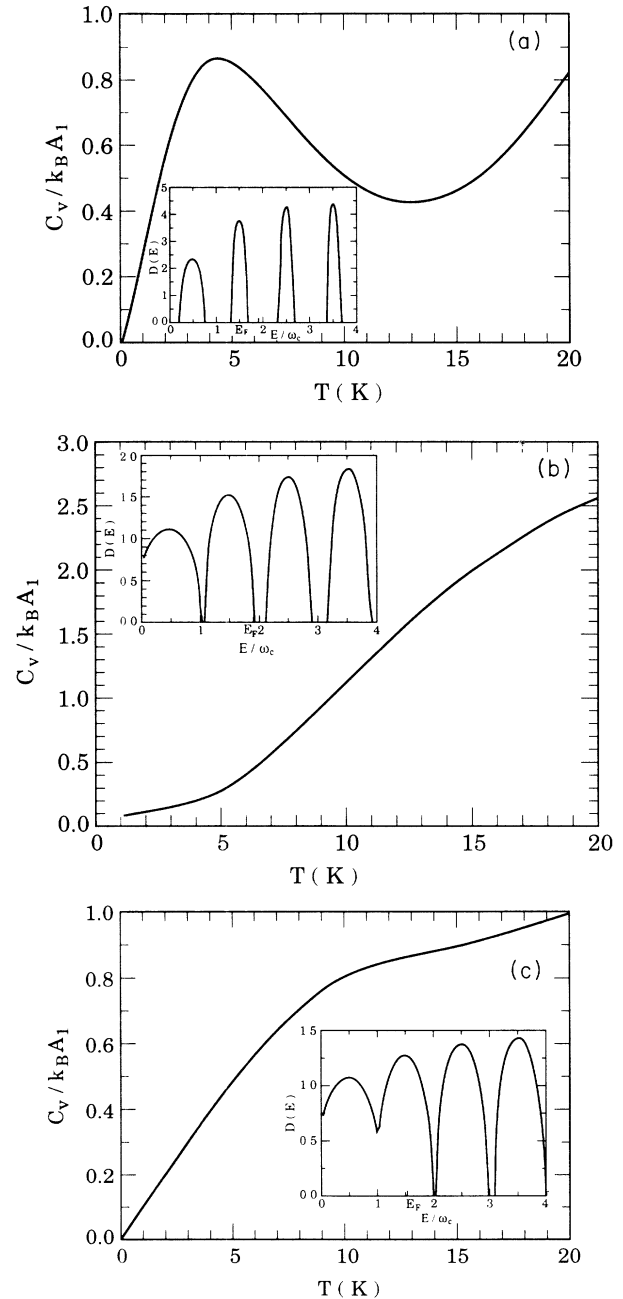


FIG. 10. The electronic specific heat C_v as a function of temperature at fixed magnetic fields (B) for three different situations: (a) $N_s = 2 \times 10^{11} \text{ cm}^{-2}$, $\mu_0 = 295\,000 \text{ cm}^2/\text{Vs}$, $B = 5.8$ T, $E_F = 1.4749\omega_c$; (b) same as in (a) except $B = 4.2$ T; $E_F = 1.8577\omega_c$ is at the edge of the Landau level; (c) $N_s = 3 \times 10^{11} \text{ cm}^{-2}$, $\mu_0 = 80\,000 \text{ cm}^2/\text{Vs}$, $B = 8$ T, $E_F = 1.5305\omega_c$. Here k_B is the Boltzmann's constant, $A_1 = eB/c$. The corresponding DOS are shown as insets in each figure.

dence of the electronic specific heat at fixed magnetic fields for three different situations: (a) $N_s = 2 \times 10^{11} \text{ cm}^{-2}$, $\mu_0 = 295\,000 \text{ cm}^2/\text{Vs}$, $B = 5.8 \text{ T}$, $E_F = 1.4749\omega_c$; (b) the same as in Fig. 10(a) except that $B = 4.2 \text{ T}$ and $E_F = 1.8577 \omega_c$ is near a Landau-level edge; (c) $N_s = 3 \times 10^{11} \text{ cm}^{-2}$, $\mu_0 = 80\,000 \text{ cm}^2/\text{Vs}$, $B = 8 \text{ T}$, $E_F = 1.5305\omega_c$. For each situation we show $D(E)$ as insets in each diagram for the same parameter set. In Fig. 11 we show the magnetic field dependence of our calculated specific heat at a fixed temperature ($T = 4.2 \text{ K}$). The self-consistent DOS $D(E_F)$ at the Fermi level is also shown as insets in Fig. 11.

The temperature dependence of C_v depends rather crucially on the location of the Fermi level and can be quite non-Fermi-liquid-like under certain conditions [Fig. 10(a)]. In Fig. 10, C_v is linear in T only up to about 3 K, beyond which pronounced nonlinearities show up. The actual regime of linear behavior depends sensitively on whether $k_B T > \Gamma$ and/or $\omega_c > k_B T$. The temperature dependence of C_v can be qualitatively understood on the basis of the detailed shape of the DOS and the position of the Fermi level with respect to the Landau levels. The linear T behavior at small T corresponds to the usual Fermi-liquid-like behavior when the chemical potential

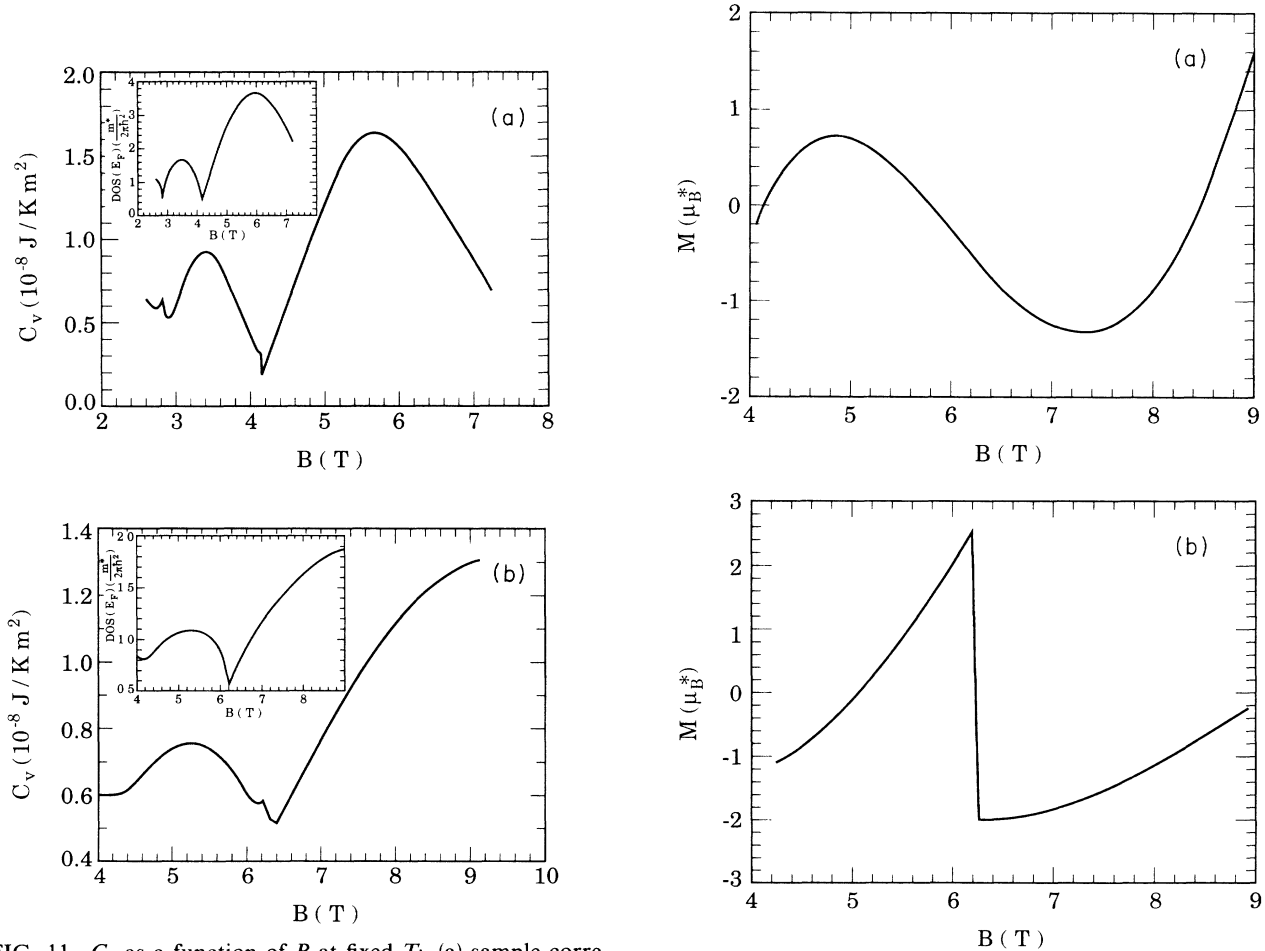


FIG. 11. C_v as a function of B at fixed T : (a) sample corresponding to Figs. 10(a) and 9(b) with $T = 4.2 \text{ K}$. (b) Sample corresponding to Fig. 10(c) with $T = 4.2 \text{ K}$. Insets of (a) and (b) show the density of states, $D(E_F)$, at the Fermi level calculated self-consistently corresponding to (a) and (b), respectively.

lies well within a broadened Landau level and mostly intra-Landau-level excitations contribute to the specific heat. As T increases, C_v eventually decreases because there is an excitation gap between the Landau levels. For even higher temperatures, however, inter-Landau-level excitations start contributing to C_v and, eventually, C_v increases with T again. Thus, C_v may show a nonmonotonic behavior [Fig. 10(a)] as a function of T for high-mobility, strong-field situations. In Fig. 11 the oscillatory behavior of C_v as a function of the magnetic field is, as one expects, very similar to the behavior of $D(E_F)$ as a function of B . There are, however, small additional structures in C_v as a function of B which arise from inter-Landau-level contributions.

Our specific-heat results agree, qualitatively, quite well with the recent experimental data of Wang *et al.*⁴ We know of no detailed attempt at observing either the non-monotonic temperature dependence of Fig. 10 or the additional structures of Fig. 11 which we predict here. We believe that these effects, even though they are small, are experimentally observable.

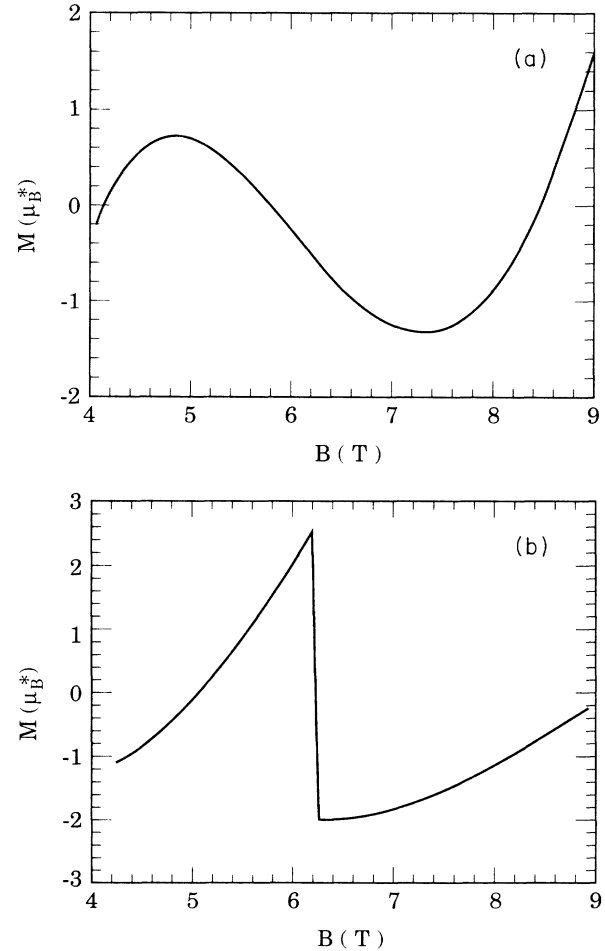


FIG. 12. The orbital magnetization M is shown as a function of the magnetic field B for the sample of Fig. 10(c) using (a) the self-consistent theory, and (b) the short-range model. μ_B^* is the effective Bohr magneton of the system.

Finally, in Fig. 12(a) we show our calculated self-consistent magnetization as a function of the magnetic field B for the same sample as shown in Figs. 10(c) and 11(b). In Fig. 12(b) we show the corresponding short-range result for the sake of comparison. Consistent with experimental findings, the variation of M with B is much less than that inferred on the basis of the short-range theory. Note that the sharp spikes in M which show up in the short-range theory are not seen experimentally. Our calculated magnetization is in excellent qualitative agreement with the existing de Haas–van Alphen measurements.²

Before concluding this section we want to discuss an aspect of the comparison between theory and experiment for the DOS and thermodynamic properties in our self-consistent model. A direct detailed quantitative comparison is simply not feasible because of the lack of accurate information about the impurity distribution in the system which determines the self-consistent DOS. We have, therefore, throughout this paper emphasized qualitative comparison between theory and experiment, stressing particularly the distinction between the well-known short-range theory and our nonlinear self-consistent theory. We feel that, given the complicated nonlinear nature of the self-consistent DOS and the fact that it depends sensitively on the impurity distribution, detailed quantitative comparisons with experimental results will not be very meaningful. We do point out, however, that to the extent we are able to make such quantitative comparison with specific experimental results we do get very good (within 10–25%) agreement. But, the important point to note is that the short-range theory is *qualitatively* wrong whereas the self-consistent theory is *qualitatively* in very good accord with experimental findings.

We conclude this section by discussing the approximations, the limitations, and the shortcomings of the self-consistent theory. We emphasize that the theory manifestly assumes a weak scattering limit so that the single-site-approximation within the SCBA is adequate to calculate the electron-impurity self-energy. This approximation is totally uncritical and, within our theory, we have no way of improving upon the SCBA or, for that matter, even to estimate the error introduced by this approximation. Secondly, we neglect all effects of electron correlation (i.e., electron-electron interaction) for the Coulomb screening introduced by the polarization bubble diagrams. The use of RPA for screening (which, however, is calculated self-consistently in the electron-impurity interaction by keeping the SCBA self-energy diagrams and the ladder vertex corrections) is also a critical approximation of the theory that we do not know how to improve upon. Thus, both of these important approximations, namely, the weak-disorder SCBA and the screening RPA, are essential approximations of our theory that cannot be relaxed. We also make some additional nonessential approximations such as assuming δ -doping for the impurity configuration so that we can parametrize the impurity distribution by only two parameters the impurity density N_i and the electron-impurity separation a , and assuming the electron layer to be perfectly two dimensional. We believe that these nonessential approxi-

mations have small effects on our calculated numerical results.

IV. CONCLUSIONS

In this paper we develop a theory for the density of states of a weakly disordered two-dimensional electron gas in the presence of a strong external magnetic field by treating scattering and screening self-consistently. Consistent with many different experimental observations, our calculated DOS is, in general, much smoother and flatter than that implied by the short-range approximation where the transport relaxation time entering the zero-field mobility completely determines the Landau-level broadening and the single-particle DOS. We find that, in addition to self-consistent screening effect (which is strongly dependent on the exact location of the chemical potential with respect to Landau-level edges), the DOS may be strongly affected by the Landau-level overlap particularly at weaker fields. Our calculated DOS cannot be parametrized by any single parameter and, in particular, zero-field mobility is qualitatively inadequate in parametrizing the strong-field DOS—we show (Fig. 3) that the same zero-field mobility could produce drastically different DOS depending on the exact impurity configuration. This is understandable since self-consistent screening depends on the details of the impurity configuration and different impurity configurations could produce the same zero-field mobility. In our model, the impurity configuration is parametrized by two parameters N_i and a , and, therefore, the DOS depends on N_i , a , N_s , and B . In real systems, one may need several more parameters to characterize the impurity distribution, consequently making the DOS dependent on more independent parameters. Thus, one unfortunate consequence of the self-consistent screening theory is the loss of simplicity of the short-range approximation where a single parameter (namely, the zero-field mobility) uniquely determines the strong-field DOS.

We use our self-consistent DOS to calculate thermodynamic properties such as the electronic specific heat and magnetization. Our calculated results are in very good qualitative agreement with experimental observations whereas calculations based on the short-range theory are in general disagreement with experimental results (as have been emphasized by many different experimental groups over the last decade). In particular, the oscillatory level broadening and the smoothness of the DOS are both verified by the experimental results. In general, the measured level broadening is substantially larger than the short-range results based on the zero-field mobility as we find in our self-consistent calculations. A word of caution about the level broadening is, however, in order. At zero magnetic field there are only two lifetimes τ_t and τ_s characterizing scattering by impurities (for short-range scattering $\tau_t = \tau_s$). For finite magnetic fields, however, the situation is more complicated and $\Gamma_N(B)$ is not uniquely determined by either τ_t or τ_s [see Figs. 6(b) and 7(b)] even though the level broadening determined by τ_s is always closer to the actual finite field result. At high magnetic fields, the short-range approxi-

mation usually works better in GaAs heterostructures.

One severe approximation of our theory is the neglect of localization which obviously plays a central role in determining the transport properties of two-dimensional systems in strong magnetic fields. One hopes that the DOS and the thermodynamic properties are insensitive to localization, although we have no way of showing that. Our current theoretical understanding of two-dimensional localization in a strong external magnetic field is based entirely¹³ on the nonlinear σ model which explicitly assumes a white-noise-type random disorder, i.e., a short-range electron-impurity potential. In this paper, on the other hand, we have been arguing that the impurity potential is anything but short range. Thus, the localization picture and the self-consistent screening picture are, at the present time, complementary and we do not know how to combine the two. We should point out

that the issue of localization in smooth, long-range potential even without a magnetic field is not yet completely solved for two-dimensional systems. Our hope is that the nonlinear self-consistency between scattering and screening which is the central idea in our theory of two-dimensional DOS remains valid even in the presence of localization. We are encouraged by the good qualitative agreement between our theory and experiment, but clearly much more work is required in this direction.

ACKNOWLEDGMENTS

This work is supported by the United States Office of Naval Research (U.S.-ONR), the United States Army Research Office (U.S.-ARO), the National Science Foundation (NSF), and the United States Department of Defense (U.S.-DOD).

¹T. Ando and Y. Uemura, J. Phys. Soc. Jpn. **36**, 959 (1974); see also T. Ando, A. B. Fowler, and F. Stern, Rev. Mod. Phys. **54**, 437 (1982).

²J. P. Eisenstein, H. L. Stormer, V. Narayanamurti, A. Y. Cho, A. C. Gossard, and C. W. Tu, Phys. Rev. Lett. **55**, 875 (1985); I. M. Templeton, J. Appl. Phys. **64**, 3570 (1988).

³E. Gornik, R. Lassnig, G. Strasser, H. L. Stormer, A. C. Gossard, and W. Wiegmann, Phys. Rev. Lett. **54**, 1820 (1985).

⁴J. K. Wang, J. H. Campbell, D. C. Tsui, and A. Y. Cho, Phys. Rev. B **38**, 6174 (1988).

⁵S. Das Sarma and X. C. Xie, Phys. Rev. Lett. **61**, 738 (1988); J. Appl. Phys. **54**, 5465 (1988).

⁶Qiang Li, X. C. Xie, and S. Das Sarma, Phys. Rev. B **40**, 1381 (1989).

⁷S. Das Sarma and F. Stern, Phys. Rev. B **15**, 8442 (1985).

⁸S. Das Sarma, Phys. Rev. Lett. **50**, 211 (1983).

⁹T. P. Smith, B. B. Goldberg, P. J. Stiles, and M. Heiblum, Phys. Rev. B **32**, 2696 (1985).

¹⁰D. Weiss, E. Stahl, G. Weimann, K. Ploog, and K. Von Klitzing, Surf. Sci. **170**, 285 (1986); M. Paalanen, D. C. Tsui, and J. C. M. Hwang, Phys. Rev. Lett. **51**, 2226 (1983); F. F. Fang, T. P. Smith, and S. L. Wright, Surf. Sci. **196**, 310 (1988); J. P. Harrang, R. J. Haggins, R. K. Goodall, P. R. Jay, M. Lavi-ron, and P. Delescluse, Phys. Rev. B **32**, 8126 (1985).

¹¹Z. Schlesinger, W. I. Wang, and A. H. MacDonald, Phys. Rev. Lett. **58**, 73 (1987); M. J. Chou, D. C. Tsui, and G. Weimann, Phys. Rev. B **37**, 848 (1988); I. V. Kukushkin and V. B. Timofeev, Surf. Sci. **196**, 196 (1988); D. Heiman, B. B. Goldberg, A. Pinczuk, C. W. Tu, A. C. Gossard, and J. H. English, Phys. Rev. Lett. **61**, 605 (1988).

¹²S. Das Sarma, Solid State Commun. **36**, 357 (1980); Phys. Rev. B **23**, 4529 (1981); R. Lassnig and E. Gornik, Solid State Commun. **47**, 959 (1983); W. Cai and C. S. Ting, Phys. Rev. B **33**, 3967 (1986); Y. Murayama and T. Ando, *ibid.* **35**, 2252 (1987).

¹³F. Wegner, Z. Phys. B **51**, 279 (1983).